CHAPTER IV

SYNTHESIS, GROWTH AND CHARACTERIZATION STUDIES OF HYDROFLUORIC ACID MIXED SULPHAMIC ACID (FASA) UV NLO CRYSTAL

4. 1. Introduction

Deep UV nonlinear optical (DUV NLO) materials garner global intense concerns owing to their ponderous technological applications in photochemistry, photoemission spectroscopy, lithography, fluorescence detection, surface-enhanced Raman scattering, communication, surgery, atto-second pulse generation etc (Shan, 2016a, Shan, 2016b). Coherent DUV light can be generated through cascades frequency conversion in NLO crystals which materialize in acentric space group and exhibit wide UV transparency with short cut-off value, moderate birefringence, large SHG efficiency higher laser damage threshold and good growth habit (Tran 2016). Primarily borates with aforesaid qualities generate UV laser (Chen 1989, Chen 1995). $KBe_2BO_3F_2$ (KBBF) is a tectonic crystal charted path to discover more DUV NLO crystals (Chen 2009). Major problems identified apically with KBBF crystal are toxic beryllium content, hard growth habit and cost effective high temperature solution growth techniques (Li 2010, Wang 2013). Recent research delineates toxic beryllium free DUV NLO crystals (Zhao 2014, Sun 2014). Soft growth habit and DUV transmittance with high SHG response were observed in thermally stable $Rb_3Al_3B_3O_{10}F$ crystal (Zhao 2015). Halide ions fortify the anisotropy in dielectric constant and ionic conductivity in nonlinear optical crystal $NaBa_4Al_2B_8O_{18}Cl_3$ (Fang 2013) and modify the dipole arrangements of chromophores in 2-amino-3-nitropyridinium halides favor for large NLO susceptibility (Chen 2014). Replacing K, Be, and F by Zn, Rb, and Cl respectively enhances the SHG response more than that of KBBF due to the cooperative effect of co parallel (BO_3) triangles and distorted

ZnO_3Cl tetrahedral (Yang 2016). Halogen influences the pervoskite frameworks of $Na_3B_6O_{10}Cl$ and $RbNa_2B_6O_{10}Cl$ to crystallize in noncentrosymmetric (NCS) space group (Bai 2015). Addition of HCl increased the mechanical stability and optical nonlinearity of L-alanine crystal (Shkir 2016). The incorporation of fluoride ion into borates and carbonates is accepted for structural distortion (Li 2014), vanishing scattering centers (Fang 2013), aligning asymmetric unit (Li 2010), photo-responsive (Ieda 2012) optical responsive (Yu 2012), blue shift effect in UV region (Zou 2013), moderate birefringence (Wang 2013) and large SHG response (Yang 2015). Fluorine assisted cation coordinates dominate on the alignment of anionic groups which are pushed to make noncentrosymmetric space group in $BaMBO_3F$ crystals (Li 2010). The orientation of fluoride anion is attributed to the large SHG response of $Ba_3B_6O_{11}F_2$ (Yu 2012). The orientation of CO_3 groups in alkali-translation metal fluoride carbonates, namely $KZnCO_3F$, $RbZnCO_3F$, $KCdCO_3F$, and RbCdCO3F was controlled by fluoride and large SHG effect was optimized (Yang 2016). Blue shift effect was produced in cadmium fluoroborate crystal $Cd_5(BO_3)F$ grown by high temperature solid state reaction method. $Cd_5(BO_3)F$ transmits UV frequencies with SHG efficiency as 4 times KDP (Zou 2013). DUV NLO crystal $GdAl_3(BO_3)_4$ was grown by top-seeded solution growth in a new flux system Al_2O_3−B_2O_3−Li_2O−NaF (Yue 2016). The growth technique employed to grow all DUV NLO crystals is based on melt growth technique. High temperature production and cost effectiveness deviate towards new growth methods.

Feasible method of mixing of various salts in solvents alleviates the synthesis of new crystalline materials (Ghazaryan 2010). Mandelic acid is mixed with water and its optical rotation in aqueous solution was studied (Levene 1929). Optical lattice modes of mixed crystal system were studied (Lucovsky 1967). Mixed crystal system

of $CdSe_yS_{1-y}$ was modelled for optically phonons (Verleur 1967). Infrared absorption was induced by impurities in mixed alkali halide crystals (Takeno 1967). Raman scattering was studied from mixed crystal system of $(Ca_xSr_{1-x})F_2$ and $(Sr_xBa_{1-x})F_2$ (Chang 1966)

Blending amino acids stoichiometrically mixed with different inorganic acids spawned very fascinate crystals (Ramasamy 2001, SrinivaFASA 2001, Karapetyan 2008). Stoichiometric mixing of HF and HNO_3 with L-arginine in aqueous solution resulted L-argininium (2+) fluoride-nitrate and di-L-argininium (2+) fluoride-hydrogen fluoride-trinitrate crystals (Ghazaryan 2013). L-Lysinium trifluoroacetate crystals were grown in aqueous solution by slow evaporation technique (Mathivanan 2008). Pr^{3+} and Yb^{3+} doped Yttrium lithium fluoride single crystals were grown by Bridgeman technique (Hu 2003). The addition of sodium fluoride (NaF) impress the growth, structural and various optical properties of ammonium dihydrogen orthophosphate (ADP) single crystals grown from aqueous solution by slow evaporation technique. The transmittance percentage is increased in the NaF doped ADP crystals and also there is an absence of characteristic absorption in the region between 340 and 1200 nm, and its SHG efficiency 1.3 times that of pure ADP crystal (Kumaresh 2016). Potassium tetra fluoro antimonate crystal ($KSbF_4$) has been synthesized using slow evaporation technique (Besky Job 2016). Spectroscopic analysis was made with difluoramine mixed with Hydrofluoric acid (Lascola 1988)

Sulphamic acid is crystallized as zwitterionic molecule ($NH_3^+SO_3^-$) of a distorted tetrahedral in the solid state but it is a strong monobasic acid in aqueous solution with $H_2N\text{-}SO_2\text{-}OH$ structure (Kanda 1951). In the zwitterionic form, the bond angles of N-S-O and O-S-O are deviated from normal tetrahedral value due to repulsive/attractive forces among negatively charged oxygen atoms and positively

charged ammonia ion. The strong lattice force due to $–NH_2$ bond accounts to its melting point is 206 º higher than other sulfonic acids. Pure sulphamic acid crystal grown by slow evaporation technique transmits UV light in the region above 258 nm (Valluvan 2006). Sulphamato based metal halogeno complexes of trivalent rhodium, iridium, ruthenium, osmium, palladium and platinum were synthesized by mixing metal-halogeno complexes with aqueous sulphamic acid solution. The sulphamato ligand binds with metal ions via the nitrogen atom rather than oxygen (Griffith 1973). Optical transmittance study on pure and metal ions doped sulphamic acid single crystals grown by slow cooling and unidirectional growth techniques (Ramesh Babu 2010). It reflects the influence of Cu^{2+}, Mn^{2+}, and Ni^{2+} ions which made the red shift in UV transparency region. Equimolar mixing of sulphamic acid with K_2CO_3 in aqueous solution yielded Potassium sulphamate single crystal at 305 K temperature by slow evaporation (Varughese 2010). Incorporation of alkali metal chlorides into sulphamic acid crystal enhanced the SHG efficiency (Pandian 2010, Thaila 2011). Doping of Ce^{3+} and Tb^{3+} enhanced the SHG efficiency of sulphamic acid (Brahmaji 2017, Brahmaji 2018). Structural modulator HF inspired us to synthesize a new mixed crystal system of hydrofluoric acid and sulphamic acid (FASA) and to characterize its structural, optical, dielectric and mechanical properties.

4. 2. Experimental Techniques

4. 2. 1. Reagents

Sulphamic acid (Amino sulphonic acid) (99% pure AR grade) and Hydrofluoric acid (99.5% pure AR grade) were purchased from E-merck Co Ltd.

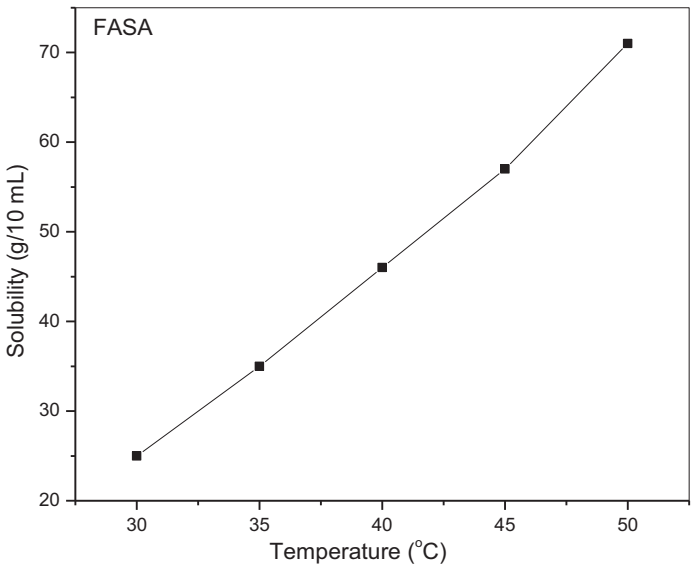

Fig. 4. 1. Solubility curve of FASA

4. 2. 2. Synthesis of FASA

Sulphamic acid was mixed with hydrofluoric acid in equimolar ratio in a 250 mL borosil glass beaker. This mixture was homogenized in water with the aid of magnetic stirrer at room temperature for 3 hrs. The resultant solution was evaporated at NTP to yield hydrofluoric acid mixed sulphamic acid (FASA) seed crystals.

4. 2. 3. Solubility study

To measure the solubility of FASA crystal in water, A 250 ml borosil glass beaker filled with 100 ml water was kept in constant temperature bath. The top of the beaker was covered with an acrylic sheet with a circular hole at the middle. A spindle from an electric motor, placed on the top of the sheet was introduced into the solution. A Teflon paddle attached at the end of the rod stirred the solution. The Crushed powder of FASA crystal was added in small amounts with water and stirring was continued till the solution attained supersaturation. A 20 ml of the saturated solution was withdrawn by means of a warmed pipette and the same was poured into a clean, dry and weighed Petri dish. The solution was kept in a heating mantle for slow evaporation till the whole of the solution got evaporated and the mass of the FASA salt in 20 ml of solution was determined by weighing the Petri dish with salt and hence the solubility, i.e quantity of salt in grams dissolved in 100 ml of the solvent was determined. The solubility of FASA in doubly deionized water was determined for five different temperatures (30, 35, 40, 45 and 50 ^{o}C) by adopting the same procedure. The resulting solubility curve of pure FASA is shown in Fig. 4. 1.

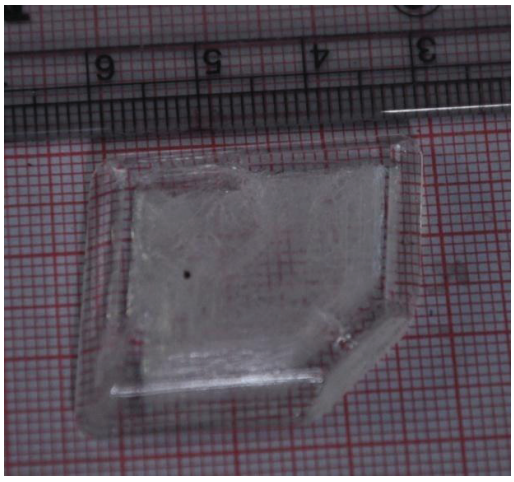

Fig. 4. 2. Photograph of as grown FASA UV NLO Crystal

4. 2. 4. Crystal growth technique

FASA crystals formed in tiny size collected from the admixture solution and dissolved in doubly deionized water with the aid of magnetic stirrer till the solution saturated. The solution was filtered through Whatman filter paper. The filtered solution was collected in a beaker and allowed for slow evaporation by covering with pored acrylic sheet at top of the beaker. After 25-30 days, all solvent dried and FASA crystal was grown at the bottom of the beaker. Fig. 4. 2 displays the FASA crystal with a size of 30 x 28 x 10 mm^3 harvested from the aqueous solution. This facile route line materialized a new novel UV NLO crystal Hydrofluoric acid admixed Sulphamic acid (FASA) grown in aqueous solution.

4. 3. RESULTS AND DISCUSSION

FASA crystal was subjected to the following studies:

i. Single crystal X-ray Diffraction analysis (XRD) for measuring unit cell parameters.

ii. X-ray Powder Diffraction analysis (XRPD) to identify the crystalline phase with crystallinity.

iii. FTIR analysis to trace out the spectral map and confirm the various functional groups present in FASA molecule.

iv. UV-Vis-NIR analysis to study the optical absorption behavior of FASA crystal and to calculate its optical band gap energy.

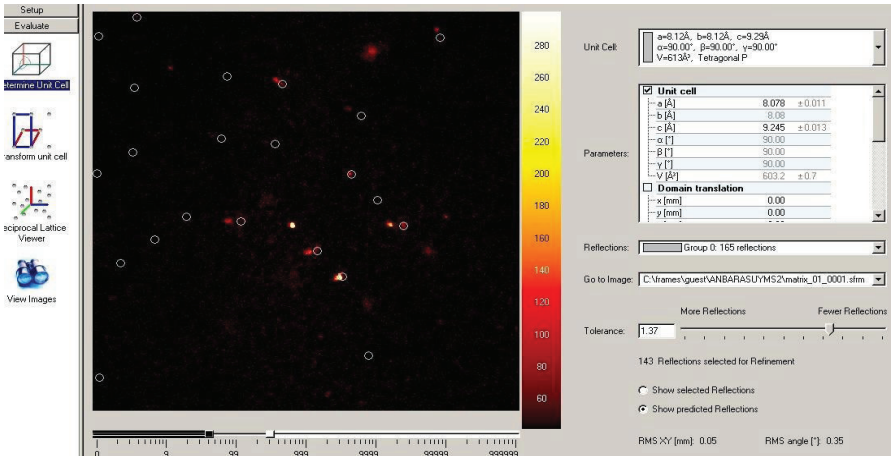

Fig. 4. 3. Single crystal XRD image of FASA UV NLO Crystal

v. Dielectric measurement technique to investigate the dielectric response of FASA for various frequency range

vi. Photoconductivity study to measure the photo responsiveness of the crystal

vii. NLO test to check the non-linear response of the crystal to the incident coherent light

viii. The phase matching between illuminated laser beams and second harmonic waves generated from FASA crystalline medium was identified.

ix. Vicker's microhardness test to study the harness of the FASA crystal

4. 3. 1 Single Crystal X-Ray Diffraction analysis

Bruker AXS Kappa Apex II CCD Diffractometer equipped with graphite monochromated Mo (Kα) (λ = 0.71073 Å) radiation diagnosed the crystal structure of FASA. A suitable size FASA crystal sample fixed at the tip of the glass fiber using cyano acrylite adhesive was mounted on the goniometer head with the aid of video microscope and optically centered at the goniometer axes. The automatic cell determination routine, with 36 frames at three different orientations of the detector was employed to collect reflections for unit cell determination. Indexing and unit cell dimensions were found out using Apex2 software by difference vector method. Fig. 4. 3 reveals FASA crystallizes in Tetragonal P crystal system with unit cell parameters of a = b = 8.12 Å, c = 9.29 Å and α=β=γ =90°, and V = 613 Å.

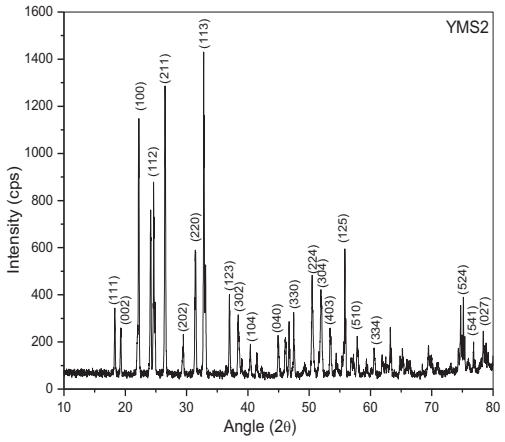

Fig. 4. 4. Powder XRD pattern of FASA UV NLO Crystal

FASA molecule ordered in tetragonal P crystal system. Pure sulphamic acid crystallized in orthorhombic system (Khanda 1951, Valluvan 2006). The influence of hydrofluoric acid modulated the structure of sulphamic acid by equalizing two lattice parameters a and b, while the other doping agents like NaCal, KCl (Thaila 2011) and metal ions (Ramesh Babu 2010) failed. The structural distortion (Li 2014) with aligning asymmetric unit (Li 2010) behavior of fluoride was attributed to the morphological changes of sulphamic acid.

4. 3. 2. Powder X-Ray Diffraction Analysis

The crushed powders of FASA crystal was subjected to powder X-ray diffraction studies with XPERT-PRO powder diffractometer. Ground sample was placed on a quartz sample holder and was mounted on the diffractometer. Cu Kα radiation of wavelength λ = 1.5418 Å illuminate the sample and the resultant diffracted beams were collected over the range of 10–80^{o} with a scan speed of 0.2^{o}/s. The crystalline phases were identified. Fig. 4. 4 displays the powder XRD pattern of FASA with various peaks, indexed manually (Hesse 1948). Crystalline planes (113), (211) and (100) diffracted with high intensity at Bragg angles of 32.7°, 26.48° and 22.15° respectively. The plane (113) diffract with FWHM of 0.0408°. The peaks observed at various Bragg's angles with different intensity confirms the FASA crystal is a distorted structure from orthogonal of pure sulphamic acid crystal (Valluvan 2006, Ramesh Babu 2010, Thaila 2011) to tetragonal. This PXRD pattern confirms the existence of mixed crystal system of hydrofluoric acid and sulphamic acid.

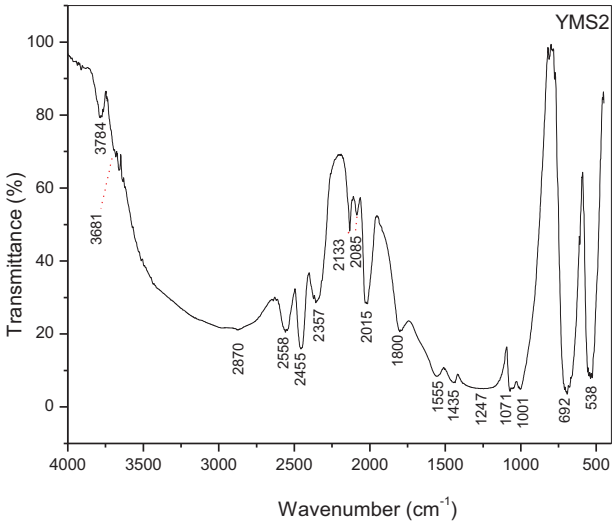

Fig. 4. 5. FTIR spectrum of FASA UV NLO Crystal

4. 3. 3. FTIR analysis

FTIR spectrometer (Bruker model IFS 66 V) evaluated the molecular functional groups present in hydrofluoric acid mixed sulphamic acid crystal. The spectrometer equipped with KBr pellet containing 0.5 mg of FASA recorded the spectra between 4000 – 400 cm^{-1}. Fig. 4. 5 depicts the FTIR spectrum exhibiting the characteristic vibrations associated with functional groups of sulphamic acid influenced by HF. A sharp peak arises at 3684 cm^{-1} is a characteristic peak of HF (Lascola 1988) incorporated into sulphamic acid host. The peak at 3660 cm^{-1} is due to SO_2-N-H stretching. The O-H stretching resonates at 1001 cm^{-1}. SO_2-OH stretching transmits the energy at 2558, 2455 and 2357 cm^{-1}. The vibrations of SO_2 stretching mode is observed at 1435, 1247 cm^{-1}. The peaks at 692 and 538 cm^{-1} are attributed to N-S stretching and SO_2 bending. N-H bending mode vibrates at 1555 cm^{-1}. Small variations and shifts in FTIR spectrum are owing to incorporation of HF which makes structure distortion.

4. 3. 4. Optical Absorption study

Varian Carry 5E model UV-vis-NIR spectrometer recorded the optical transmittance against the wavelengths of UV-vis-NIR region from 200 nm to 1400 nm. Fig. 4. 6 depicts the optical transmittance spectrum showing FASA emanate UV radiation from 200 nm with short cut-off value found very close to 200 nm. Wavelength increases from 200 nm to 210 nm, transmittance percentage exponentially increases from 45 to 85%. It was estimated on the transmittance that there is a possibility to obtain cut-off value shorter than 200 nm. The doping of Ce^{3+} ion made red shift in UV transmittance of pure sulphamic crystal with lower cut off 340 nm (Brahmaji 2017).

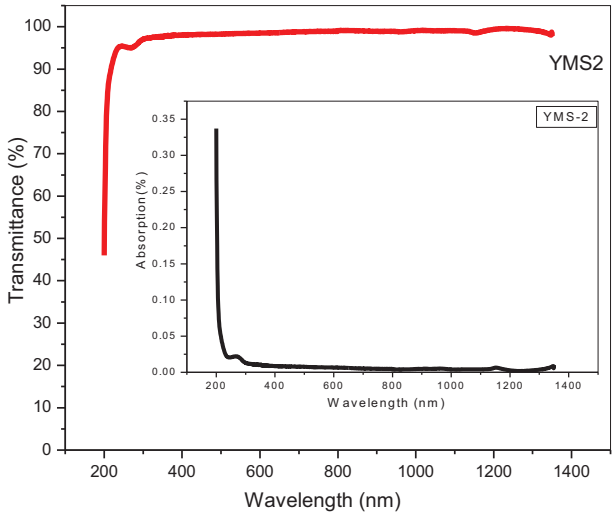

Fig. 4. 6. Optical transmittance of FASA UV NLO Crystal. The insert is the absorbance spectrum

Tb^{3+} doped sulphamic acid single crystals (Brahmaji 2018) with low cut off wavelength 259 nm. The doping of Cu^{2+}, Mn^{2+}, and Ni^{2+} ions decreased UV transmittance of pure sulphamic crystal with lower cut off around 270 nm (Ramesh Babu 2010) . But the incorporation of optical responsive HF into sulphamic acid host made a blue shit in UV transmittance (Yu 2012, Zou 2013) and wider optical window.

The band gap of the material E_g sets the limiting cut-off wavelength λ_c defined by $\lambda_c = hc/E_g$, where h is the Planck's constant and c is the velocity of the light. The optical band gap E_g from Tauc's expression is

$$(\alpha h\nu)^n = A(h\nu - E_g) \qquad \text{---------- (1)}$$

where α is the absorption coefficient, n = 2 for direct transition and n=1/2 for indirect transition. The parameter A is a constant. E_g is calculated from the plot of $(\alpha h\nu)^n$ against hν. α was determined from the Transmittance using the relation

$$\alpha = (2.303/t)*\log(1/T) \qquad \text{---------- (2)}$$

where t is the sample thickness and T is the Transmittance. The direct optical band gap energy was found to be 5.95 eV from Fig. 4. 7 and the indirect optical band gap energy was found to be 5.59 eV from Fig. 4. 8. The optical band gap energy of $KSbF_4$ crystal has been estimated as 4.84 eV. In the UV region, optical conductivity has very high values of the order of 10^{13} S^{-1} and in the visible region it is of the order of 10^8 S^{-1} (Besky Job 2016). The direct band gap energy of Ce^{3+} doped SA is calculated as 4.6 eV (Brahmaji 2017). The direct band gap energy of Tb^{3+} doped sulphamic acid is calculated as 4.2 eV (Brahmaji 2018).

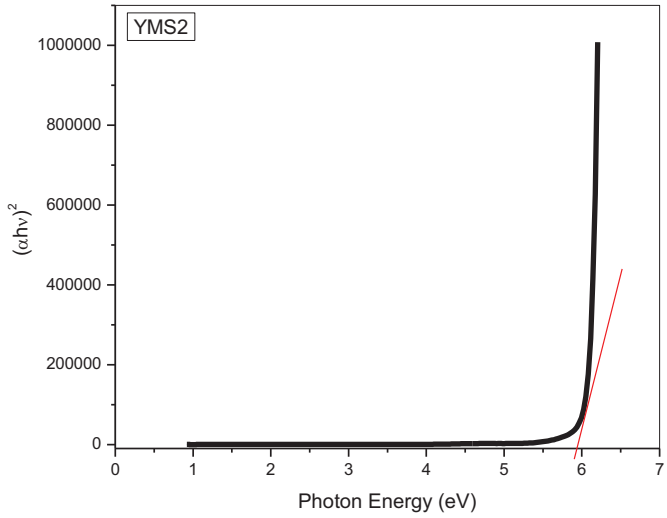

Fig. 4. 7. Tauc's Plot for direct optical band gap energy of FASA UV NLO Crystal

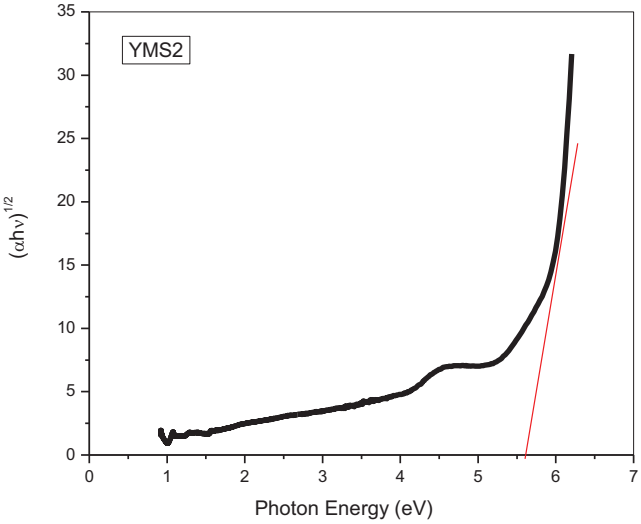

Fig. 4. 8. Tauc's Plot for indirect optical band gap energy of FASA UV NLO Crystal

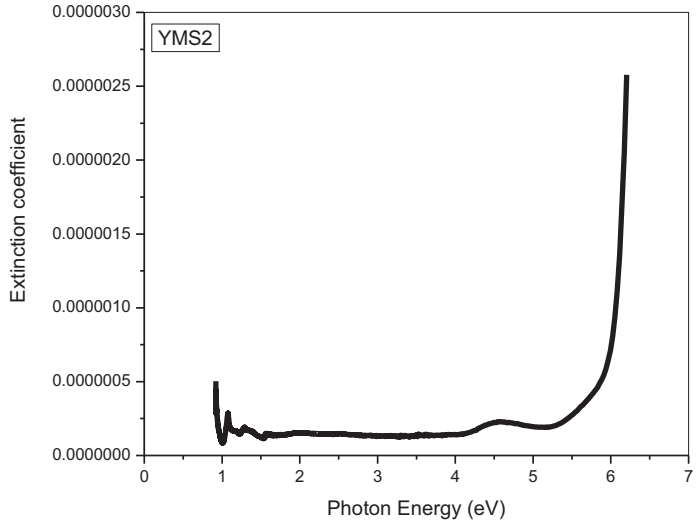

Fig. 4. 9. Plot of Extinction coefficient of FASA UV NLO Crystal

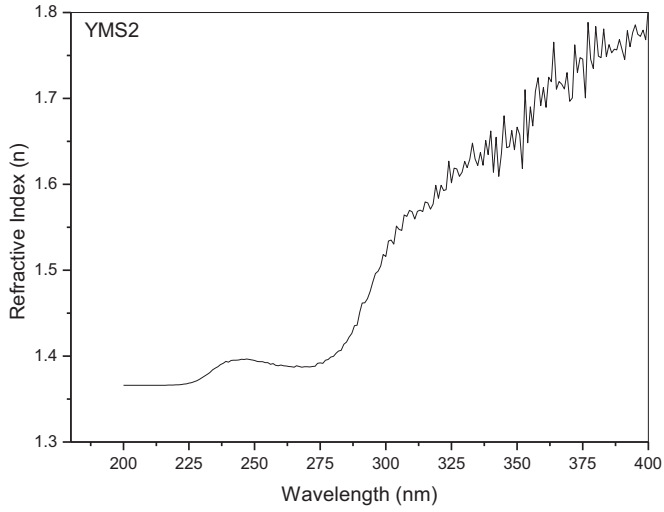

Fig. 4. 10. Plot of Refractive Index of FASA UV NLO Crystal

The optical band gap energy of FASA higher than other sulphamic acid based crystals. The other optical constants like extinction coefficient and refractive index are calculated from the formula reported earlier (Vadivel 2018). The extinction coefficient of FASA crystal was plotted against the energy as shown in Fig. 4. 9 and the refractive index was plotted against wavelength as shown in Fig. 4. 10. FASA exhibits low extinction coefficient and low refractive indices in UV region. The refractive indices of FASA in UV region are lower than that of a UV NLO crystal $NaSr_3Be_3O_9F_4$ (Wang 2013). Wider UV transmittance window with low refractive index, low extinction coefficient and high optical band cap energy make FASA suitable for various optical applications.

4. 3. 5. Dielectric studies

Dielectric measurements for silver coated FASA crystal sample was carried out in the frequency range of 50 Hz to 5 MHz using Hioki 3532-50 LCR Hitester at various temperatures (40, 50, 60 ,70 ^{o}C). The plots of dielectric constant (ε_r) and dielectric loss (D) were drawn against frequency (log f) for different temperatures as shown in Fig. 4. 11 & Fig. 4. 12 respectively. FASA molecules polarized more when local electric field of low frequency induced them, due to the sum of space charge, dipolar, ionic and electronic polarizability. As the frequency of electric field increases, charge, dipolar, ionic polarizability became ineffective except electronic polarizability and the relative permittivity of FASA decreases as well as dielectric loss. This normal dielectric sense of FASA discloses its charge transport mechanism and electric field distribution at all temperatures. The maximum values of dielectric constant of FASA are 2.46, 0.66, 1.6 and 5.91 at 40, 50, 60 and 70 ^{o}C respectively.

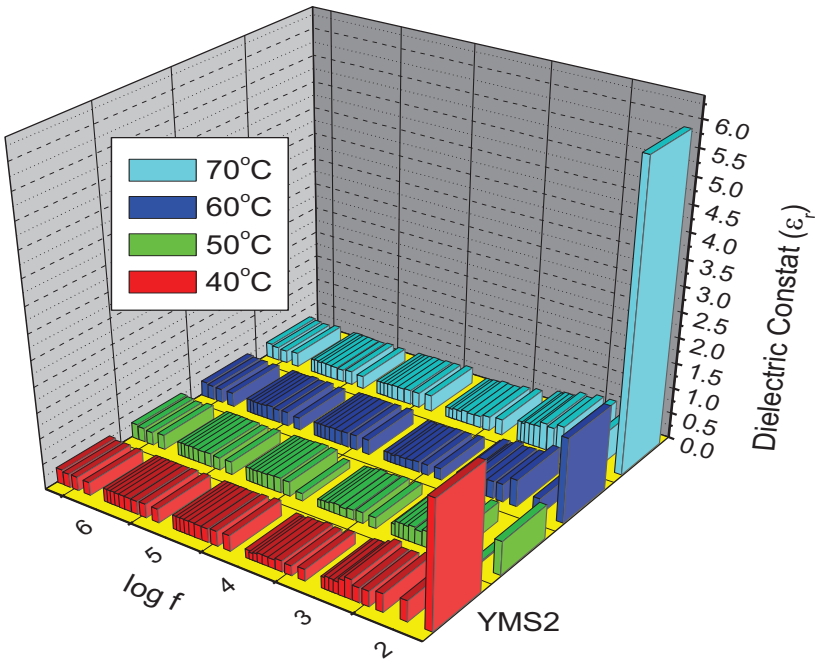

Fig. 4. 11. Plot of Dielectric constant of FASA UV NLO Crystal

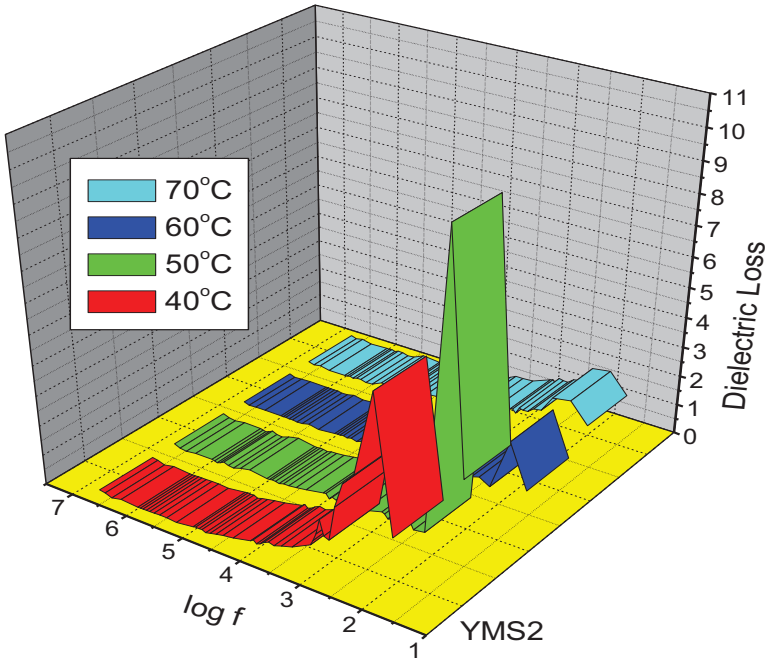

Fig. 4. 12. Plot of Dielectric loss of FASA UV NLO Crystal

The maximum values of dielectric loss (D) of FASA are 6.56, 9.99, 1.89 and 1.75 at 40, 50, 60 and 70 ^{o}C respectively. For the dielectric constant was high, the dielectric loss was minimum. The normal dielectric behavior was studied in metal ions doped sulphamic acid (Ramesh Babu 2010) and in Ce^{3+}, Tb^{3+} doped sulphamic acid (Brahmaji 2017, Brahmaji 2018).

4. 3. 6. Photoconductivity study

Keithley 485 pico ammeter measured the photoconductivity FASA samples. Initially, the sample was kept away from any other radiations. The crystal sample was connected in series to a DC power supply and pico ammeter. Silver paint was coated on sample to make the electrical contacts. The radiation from a halogen lamp containing iodine vapour was exposed on the sample by focusing a spot of light on the sample with the help of a convex lens. The photocurrent (I_p) was calculated. Initially the applied voltage was increased from 0 to 100 V in steps of 20 V and the corresponding dark currents were measured. Fig. 4. 13 shows the plot of variation of both the dark current and photo current of the sample against the applied voltage. Both the dark and photocurrent were seen to increase linearly with the applied field. For the same applied field, the photo current is less than the dark current which reveals the negative photo conducting behaviour of FASA single crystal. The $KSbF_4$ crystal shows negative photo conductivity (Besky Job 2016).

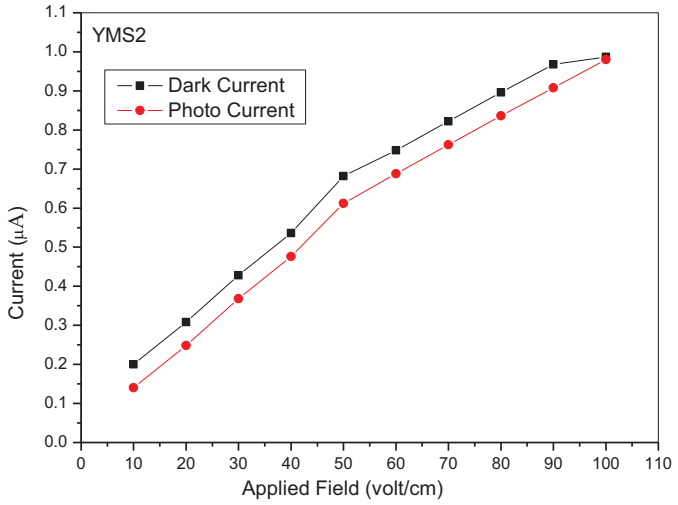

Fig. 4. 13. Photoconductivity of FASA UV NLO Crystal

4. 3. 7. NLO Test

In Kurtz-Perry powder test, Nd: YAG laser having fundamental radiation of 1064 nm with an input power 0.68 J as the optical source and illuminated on to the powdered sample of FASA through a visible blocking filter. a monochromator collected the 532 nm radiation after spreading the 1064 nm pump beam with an infrared blocking filter. FASA emanated second harmonics of primary Nd:YAG laser. Powder SHG efficiency was measured by a photomultiplier tube. A sample of KDP was used as a reference material for the present measurement. It is found that the FASA single crystal has an efficiency of 0.43 times that of KDP. It is greater than that of some DUV NLO crystals KBBF (Wu 1996).

4. 3. 8. Phase Matching study

FASA crystalline sample was ground and sieved into distinct particle sizes in the range of less than 106, 106-125, 125-150 and above 150 μm. KDP crystal was also sieved into the particle dimension of FASA. Q-switched Nd:YAG infrared laser pulses irradiated on the sieves. SHG efficiency depends on the particle size and varies with size of sieves. SHG output was measured and plotted for various particle size. SHG intensities increased with increasing particle size upto 150 μm as shown in Fig. 4. 14. It proves the phase matching behavior of FASA. It is a promising phase matchable NLO crystal for LASER generation.

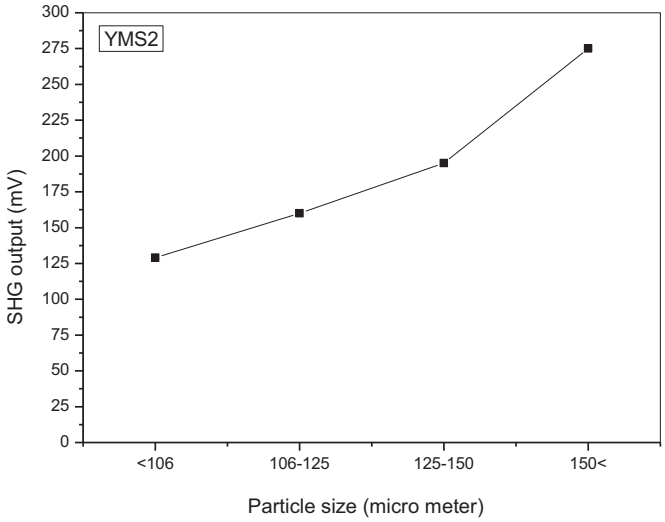

Fig. 4. 14. Phasematching curve of FASA UV NLO Crystal

4. 3. 9. Microhardness Test

Leitz Wietzlar Vickers Microhardness tester measured the hardness parameters of single crystal of FASA at room temperature. Flat shape crystal was fitted with a Vickers diamond pyramidal indenter light microscope. The static indentations were made at room temperature with a constant indentation time of 15 seconds for all indentation. The indenter marked on the crystal surfaces by varying the load from 20 to 100 g. The Vickers microhardness number H_v of the crystal was calculated using the relation

$$H_v = 1.8544\ P/d^2\ Kg\ mm^{-2} \quad \text{---------- (3)}$$

where P is the applied load and d is the average diagonal length of the indented impression in mm. Vickers microhardness profile as a function of load is shown in Fig. 4. 15. (a)

By using Meyer's law, the load P is related with the indentation size as

$$P = k_1 d^n \quad \text{---------- (4)}$$

Mayer constant (k_1) and work hardening coefficient (n) are the constants for a particular sample. The work hardening coefficient n is calculated from the slope of the curve drawn by plotting log (P) against log (d) as shown in Fig. 4. 15 (b)

The value of k_1 was measured from the derivative of the curve drawn by plotting P against d^n as shown in Fig. 4.14 (c). The value of n is found to be 2.45.

If n is greater than 2, the microhardness number H_v increases with increasing load (Onitsch 1947, Hanneman 1941), The work hardening coefficient value of FASA proves that FASA is a soft material.

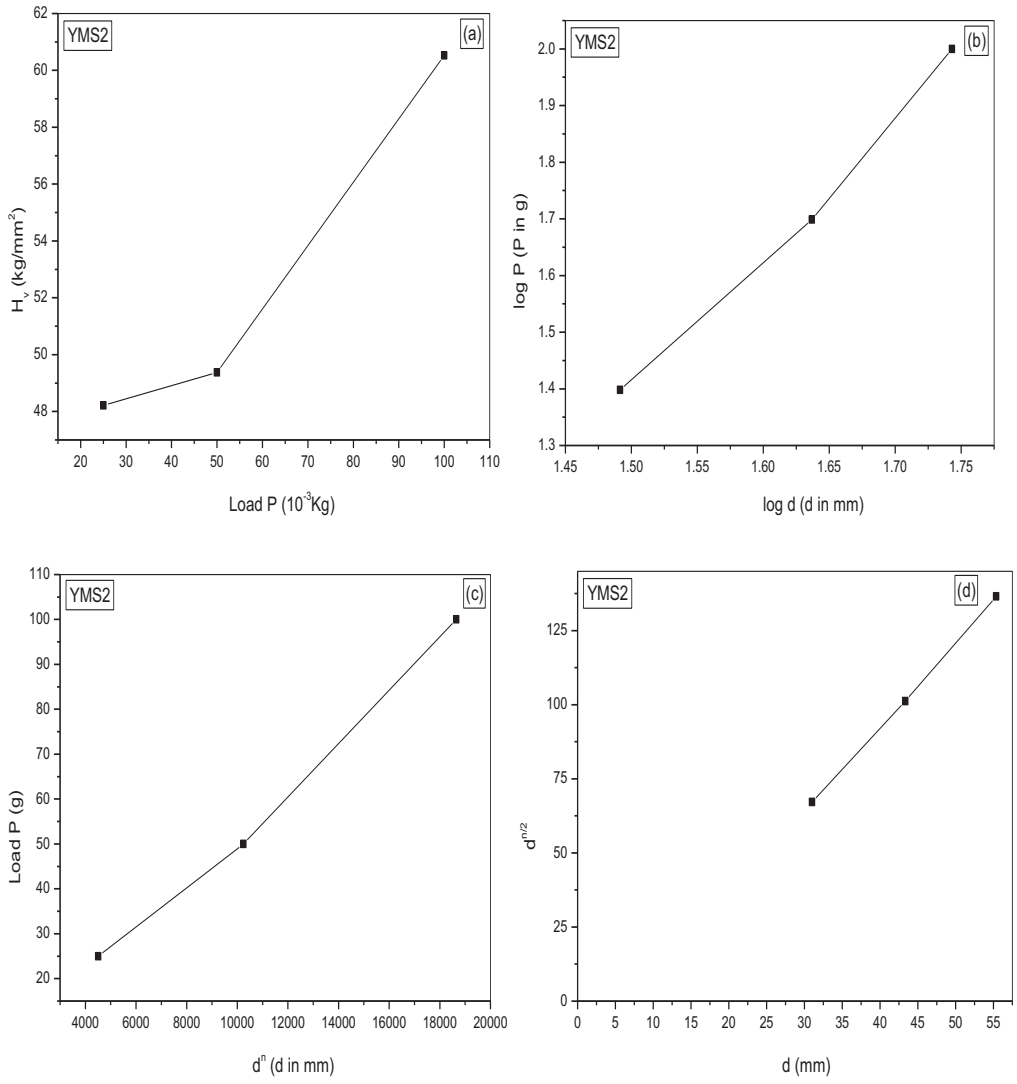

Fig. 4. 15. Microhardness measurements of FASA UV NLO crystal. (a) Variation of harness with load, (b) Plot of log P versus log d, (c) Plot of d^n versus P, (d) Plot of d versus $d^{n/2}$.

Table 4. 1. Hardness Parameters of FASA UV NLO Crystal

Hardness Parameters	Calculated Value
N	2.45
k_1	5.15 (10^{-3} Kg)
k_2	41.83 (10^{-3} Kg)
X	7.5 (μm)
σ_v	13.93 (MPa)

The degree of dislocation density of the material is related with load P and indentation d through Kick's law given by

$P = k_2(d+x)^2$ ---------- (5)

By simplifying Eqn. (4) and (5) we get

$d^{n/2} = (k_2/k_1)^{1/2} d + (k_2/k_1) x$ ---------- (6)

$d^{n/2}$ is plotted against d as shown in Fig. 4.15(d) and the slope of the straight line yields $(k_2/k_1)^{1/2}$ and the intercept is a degree of x.

The yield strength of the material is given by

$\sigma_v = (H_v/2.9)\{[1-(2-n)] \times [(12.5)(2-n)/(1-(2-n))]^{2-n}\}$ ---------- (7)

From the graphs, the constants k_1, k_2 and x are evaluated and the yield strength (σ_v) of FASA is computed. Hardness parameters of FASA crystal are tabulated in Table 4.1. As the work hardening coefficient value of FASA is n=2.45, it suggests that FASA is a soft material. The incorporation of Fluorine supported the soft growth habit and made it feasible to process.

4. 4. Conclusion

Hydrofluoric acid mixed Sulphamic acid crystal (FASA) was grown in aqueous solution by slow evaporation technique. The incorporation of fluorine equalized the two lattice axis of sulphamic acid host molecule and FASA crystallized in Tetragonal crystal system. The presence of fluorine and other functional groups of sulphamic acid were confirmed by FTIR spectroscopy technique. Wider UV transmittance window starts from near 200 nm. The optical band gap energy of FASA is 5.95 eV. UV light could travel through FASA crystal faster. The dielectric sense of FASA molecules was confirmed. FASA was negative photoconductor. It is a phase matchable second order NLO crystal. Its SHG efficiency was calculated as 0.43 times of KDP. Soft crystal growth habit made it feasible to process. FASA is a UV transmittable crystal suitable for various energy harvesting processes.